Tridirectional protonic conductivity in soft materials

M„ki-Ontto, R.; de Moel, K.; Polushkin, Evgeny; Alberda van Ekenstein, G.O.R.; ten Brinke, G.; Ikkala, O.; Mäki-Ontto, Riikka; Maki-Ontto, R

Published in:
Advanced Materials

DOI:
10.1002/1521-4095(20020304)14:5<357::AID-ADMA357>3.0.CO;2-Q

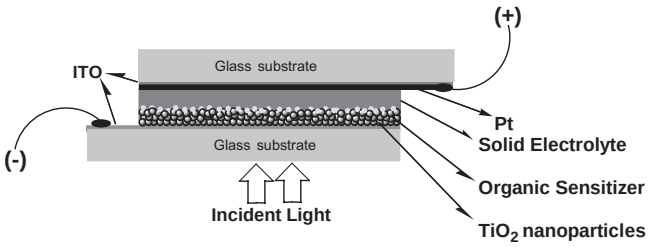

Fig. 4. Schematic cross section of the DSPEC.

ATR IR spectra were measured on a Fourier transform infrared (FTIR) Perkin-Elmer System 2000 spectrometer equipped with a SpectraTech horizontal ATR cell (60° incident angle, Ge ATR crystal).

Titanium dioxide mesoporous films were deposited on ITO glass by the reverse-micellar route and the photosensitizer $RuL_2(NCS)_2$ was attached as in [3]. The ureasil precursors were synthesized as in [18]. Synthesis of class II nanocomposite gels using ureasil precursors, their enrichment with the iodine/iodide couple, and their deposition in a DSPEC was carried out as follows: absolute ethanol (2 mL) was mixed with the ureasil precursor (PP-4000, 2 g). KI (0.5 M) and I_2 (0.05 M) were added to the above mixture with stirring at ambient conditions. The mixture was continuously stirred for about 3 h. Then acetic acid (0.35 mL) was added and stirring continued for another 4 h at ambient conditions. At the end of this period, a viscous brown fluid was obtained. A few drops of this solution were applied to the electrode-bearing TiO_2 film with attached dye and we placed the second (platinized) electrode on top, simply by pressing the two electrodes together. Connections were made with silver paste and a copper ribbon as seen schematically in Figure 4.

Received: October 29, 2001
Final version: November 30, 2001

[1] B. O'Reagan, M. Grätzel, *Nature* **1991**, *353*, 737.
[2] M. K. Nazeeruddin, A. Kay, I. Rodicio, R. Humphry-Baker, E. Müller, P. Liska, N. Vlachopoulos, M. Grätzel, *J. Am. Chem. Soc.* **1993**, *115*, 6382.
[3] E. Stathatos, P. Lianos, C. Krontiras, *J. Phys. Chem.* **2001**, *105*, 3486.
[4] B. O'Reagan, D. T. Schwartz, *J. Appl. Phys.* **1996**, *80*, 4749.
[5] F. Cao, G. Oskam, C. P. Searson, *J. Phys. Chem.* **1995**, *99*, 17 071.
[6] M. Matsumoto, H. Miyazaki, K. Matsuhiro, Y. Kumashiro, Y. Takaoka, *Solid State Ionics* **1996**, *89*, 263.
[7] K. Tennakone, G. K. R. Senadeera, V. P S. Perera, I. R. M. Kottegoda, L. A. A . De Silva, *Chem. Mater.* **1999**, *11*, 2474.
[8] A. F. Nogueira, J. R. Durrant, M. A. De Paoli, *Adv. Mater.* **2001**, *13*, 826.
[9] K. Murakoshi, R. Kogure, Y. Wada, S. Yanagida, *Sol. Energy Mater. Sol. Cells* **1998**, *55*, 113.
[10] J. Hagen, W. Schaffrath, P. Otschik, R. Fink, A. Bacher, H.-W. Schmidt, D. Haarer, *Synth. Met.* **1997**, *89*, 215.
[11] A. C. Arango, L. R. Johnson, V. N. Bliznyuk, Z. Schlesinger, S. A. Carter, H.-H. Horhold, *Adv. Mater.* **2000**, *12*, 1689.
[12] M. M. Gomez, J. Lu, E. Olsson, A. Hagfeldt, C. G. Granqvist, *Sol. Energy Mater. Sol. Cells* **2000**, *64*, 385.
[13] V. Bach, D. Lupo, P. Comte, J. E. Moser, F. Weissoertel, J. Salbeck, H. Spreitzer, M. Grätzel, *Nature* **1998**, *395*, 583.
[14] B. O'Reagan, D. T. Schwartz, *Chem. Mater.* **1998**, *10*, 1501.
[15] B. O'Reagan, D. T. Schwartz, S. M. Zakeeruddin, M. Grätzel, *Adv. Mater.* **2000**, *12*, 1263.
[16] A. F. Nogueira, M. A. De Paoli, *Sol. Energy Mater. Sol. Cells* **2000**, *61*, 135.
[17] P. Judeinstein, C. Sanchez, *J. Mater. Chem.* **1996**, *6*, 511.
[18] E. Stathatos, P. Lianos, U. Lavrencic-Stangar, B. Orel, P. Judeinstein, *Langmuir* **2000**, *16*, 8672.
[19] U. Lavrencic-Stangar, N. Groselj, B. Orel, P. Colomban, *Chem. Mater.* **2000**, *12*, 3745.
[20] E. J. A. Pope, J. D. Mackenzie, *J. Non-Cryst. Solids* **1986**, *87*, 185.
[21] A. L. Smith, *Spectrochim. Acta* **1960**, *16*, 87.
[22] L. J. Bellamy, *The Infrared Spectra of Complex Molecules*, Chapman and Hall, London **1975**, Ch. 20.
[23] E. Stathatos, P. Lianos, A. Laschewsky, O. Ouari, P. Van Cleuvenbergen, *Chem. Mater.* **2001**, *13*, 3888.
[24] K. Kalyanasundaram, M. Grätzel, *Coord. Chem. Rev.* **1998**, *77*, 347.

Tridirectional Protonic Conductivity in Soft Materials**

By *Riikka Mäki-Ontto*, *Karin de Moel*, *Evgeny Polushkin*, *Gert Alberda van Ekenstein*, *Gerrit ten Brinke*,* and *Olli Ikkala**

Hierarchical polymeric materials, with *structure-within-structure* morphologies, have attracted interest due to their potential as functional materials.[1] For this work, we constructed an assembly of nanoscale protonically conducting "wires" using hierarchical self-organization of polymeric supramolecules. The supramolecules consist of poly(styrene)-*block*-poly(4-vinyl pyridine), PS-*block*-P4VP, where the latter block forms a stochiometric acid–base complex with toluene sulfonic acid (TSA), which is in turn stochiometrically hydrogen bonded with 3-*n*-pentadecylphenol (PDP), to form PS-*block*-$P4VP(TSA)_{1.0}(PDP)_{1.0}$, Scheme 1. In an effort to achieve "a monodomain", the local structures are aligned

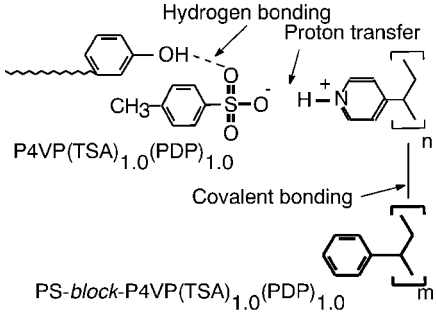

Scheme 1.

globally by shear flow and the conductivity is enhanced. Protonic transport is macroscopically tridirectional, and largest along the "wires", both below and above the glass transition point. The nanoscale structures thus allow tuning of the protonic conductivity and anisotropy in soft materials once the structures have been globally aligned.

Electroactive polymers range from conjugated polymers[2] to ionic and protonic conducting[3] materials. They allow conceptually new applications to be realized with a flexibility of the products, as well as new processing and design opportu-

[*] Prof. O. Ikkala, Dr. R. Mäki-Ontto
Department of Engineering Physics and Mathematics
Helsinki University of Technology
FIN-02015 HUT, Espoo (Finland)
E-mail: Olli.Ikkala@hut.fi
Prof. G. ten Brinke, Dr. K. de Moel, Dr. E. Polushkin,
G. Alberda van Ekenstein
Laboratory of Polymer Chemistry and Materials Science Center
Dutch Polymer Institute, University of Groningen
NL-9747 AG Groningen (The Netherlands)
E-mail: G.ten.Brinke@chem.rug.nl

[**] This work has been supported by the Finnish Academy and Technology Development Center (Finland). K. de M. gratefully acknowledges financial support from the DSM within the Computational Materials Science program of the Dutch Society for Scientific Research (NWO). Tapio Mäkelä is acknowledged for instructions in the electrical measurements.

  0935-9648/02/0503-0357 $ 17.50+.50/0

ADVANCED MATERIALS

nities. Self-organization involving conducting or conjugated domains has been studied earlier, based on block copolymers[4–13] and hairy rods.[14–17] More recently, undoped hairy rods[18,19] and the corresponding doped hydrogen-bonded supramolecules[20] have shown attractive transport properties. For ionic conductivity, solid polymer electrolytes involving lithium salts have aroused major interest, where suppression of the host polymer's crystallization increases the conductivity; block copolymers have been used as the suppressing agent.[21,22] More recently, the possibilities for nanoscale structures, using the self-organization of block copolymer, hairy-rod type, or liquid crystalline substances, have been reported for lithium conductors.[23–29] Finally, perfluorinated polymeric sulfonic acids are promising materials for protonic conductors,[3,30] where the conductivity is due to proton hopping along adsorbed water molecules.[31,32] Interesting results have been found for polyelectrolyte surfactant complexes, where an ohmic to non-ohmic conductivity change is observed.[33,34] Another major type of protonically conducting polymers consists of acid–base complexes, such as salts of sulfonic-acid containing polymers blended with basic polymers.[35,36] Acid–base complexes are specifically studied in this work.

In protonic conductors, the potential of self-organization within the polymeric host has not been discussed extensively, although self-organization might allow confinement of the moieties involved in the proton hopping (and also water molecules) in tailored and stable nanoscale channels. Previously, we reported that polymeric supramolecules (and supramolecules in general[37]) could be formed by hydrogen-bonding of alkyl phenols (such as PDP) to P4VP, which itself was complexed with methane sulfonic acid.[38] Such supramolecules self-organize to form lamellar structures. If the P4VP chains are further covalently connected to PS blocks, an additional length scale is introduced, to render *lamellar-within-lamellar* structures.[38] In such materials, a sequence of phase transitions as a function of temperature allows protonic conductivity to be switched.

We report here on the construction of protonically conducting acid–base complexes to form self-organized polydomain nanostructures, manipulation of the structures by shear flow[39–43] to aim for a monodomain structure, and show that the macroscopically aligned nanostructure with fewer domain boundaries, namely less defects, is directly reflected in the transport of protons. The final result leads both to a considerably improved conductivity and to tridirectionality of the macroscopic conductivity anisotropy.

An acid–base complex is formed between P4VP and a stoichiometric amount of TSA. This choice was motivated by two factors. Firstly, the acid–base complexes between several basic polymers, including P4VP, with polymeric sulfonic acids allow relatively high protonic conductivity both in the hydrated and dehydrated state.[35,36] In this work, we preferred oligomeric sulfonic acids, as we expected more perfect structures in this case. Secondly, TSA was selected because its aromatic nature allows enhanced thermal stability to be obtained. A stoichiometric amount of PDP versus sulfonate groups was taken to form the hydrogen-bonded comb-shaped complex (Scheme 1). The P4VP was included also as one block of a diblock copolymer PS-*block*-P4VP with weight fraction of PS f_{PS} = 0.88. Assuming that TSA and PDP are nominally fully complexed to form the supramolecules PS-*block*-P4VP(TSA)$_{1.0}$(PDP)$_{1.0}$ (Scheme 1), the weight fraction of the PS block is f_{PS} = 0.62. This value suggests self-organized alternating lamellae of PS and P4VP(TSA)$_{1.0}$(PDP)$_{1.0}$ (and related materials[38,44]). Our previous studies[38,44] suggest that within the P4VP(TSA)$_{1.0}$(PDP)$_{1.0}$ layers, there will be another "inner" level of self-organization, which consists of alternating layers of non-polar pentadecyl chains and polymeric salt moieties. The expected scheme of self-organization is shown in Figure 1B. That such structures really were achieved will be demonstrated later by small-angle X-ray scattering (SAXS), see Figure 2.

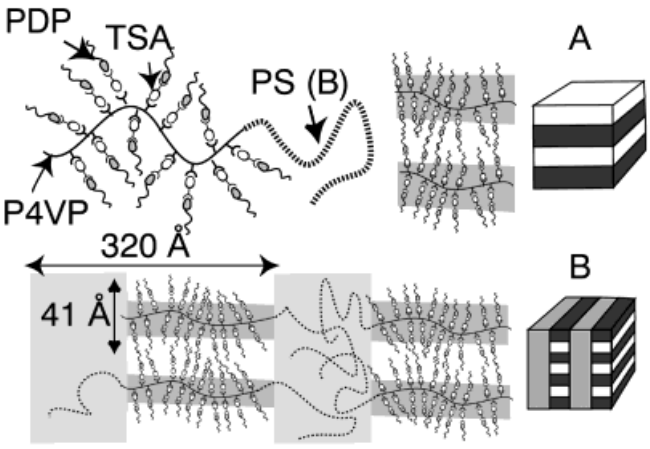

Fig. 1. Representation of the self-organized structures based on the acid–base protonic conductor P4VP(TSA)$_{1.0}$. A) P4VP(TSA)$_{1.0}$(PDP)$_{1.0}$: two-dimensional (lamellar) nanoscale conducting lamellae formed upon hydrogen bonding between P4VP(TSA)$_{1.0}$ and pentadecyl phenol (PDP). B) PS-*block*-P4VP(TSA)$_{1.0}$(PDP)$_{1.0}$: Essentially one-dimensional protonically conducting nanoscale wires are present. The hierarchical self-organization due to covalent bonding between P4VP and PS to form a block copolymer and the hydrogen bonding of P4VP(TSA)$_{1.0}$ to PDP are indicated.

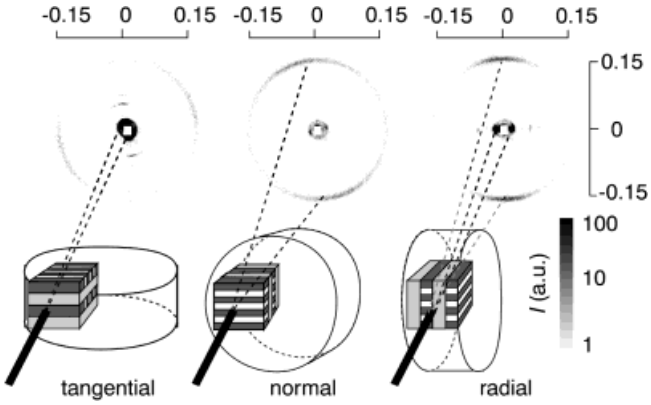

Fig. 2. Flow-induced overall alignment of the protonically conducting nanoscale wires of PS-*block*-P4VP(TSA)$_{1.0}$(PDP)$_{1.0}$ after shearing at 0.1 Hz and 100 % strain amplitude at 140 and 110 °C, both for 8 h. The corresponding two-dimensional SAXS intensities in the tangential, normal, and radial directions are shown. The scale is in 1/Å units.

  0935-9648/02/0503-0358 $ 17.50+.50/0

The self-organized nanoscale structures are local structures and additional driving forces, such as a shear flow field,[39,40,42,43] electric field,[45] or surfaces,[46] have to be invoked to achieve macroscopic alignment when striving towards monodomains. Figure 2 shows the two-dimensional SAXS intensity patterns of a flow-oriented sample in the tangential, normal, and radial directions. Scattering peaks are observed at q_1 = 0.02 Å^{-1} and $2q_1$, which indicates a lamellar self-organization between PS and P4VP(TSA)$_{1.0}$(PDP)$_{1.0}$ with a periodicity of 320 Å. The lamellae are relatively well aligned along the shearing planes, see Figure 2. SAXS also shows another peak at q_2 = 0.15 Å^{-1}. The second-order peak is beyond the range shown in Figure 2. However, from the corresponding homopolymeric supramolecules P4VP(TSA)$_{1.0}$-(PDP)$_{1.0}$ (see Fig. 3), the structure can be assigned to a lamellar order with a long period of 41 Å, as shown in Figure 1B. Importantly, this structure, corresponding to the orientation of the protonically conducting nanowires, becomes globally relatively well oriented after the imposed flow, as shown in Figure 2.

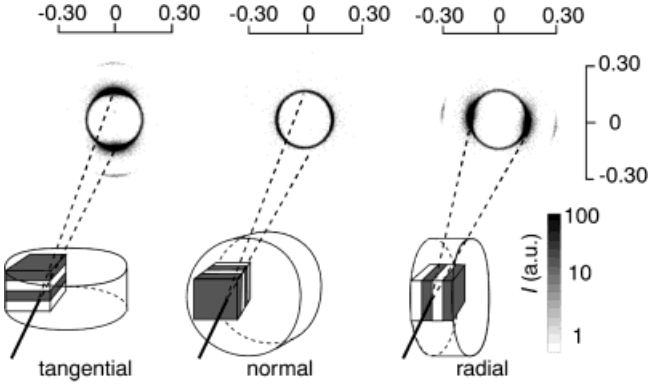

Fig. 3. The flow-induced overall alignment of the protonically conducting lamellae of P4VP(TSA)$_{1.0}$(PDP)$_{1.0}$ after shearing at 0.1 Hz and 100 % strain amplitude at 110 °C for 8 h. The corresponding two-dimensional SAXS intensities in the tangential, normal, and radial directions are shown. The scale is in 1/Å units.

The conductivities were investigated using the simple Arrhenius and empirical Vogel–Tamman–Fulcher (VTF) equations, which are widely used for crystalline and amorphous polymer electrolytes.[47–50] The inset of Figure 4 shows the conductivity of the pristine acid–base complex P4VP(TSA)$_{1.0}$. The conductivity is poor and obeys the Arrhenius equation

$$\sigma(T) = A \exp(-E_\sigma/kT) \quad (1)$$

with activation energy $E_\sigma \approx$ 1.8 eV. Figure 4 shows that the conductivity of PS-*block*-P4VP(TSA)$_{1.0}$(PDP)$_{1.0}$ is drastically higher due to plasticization, even without alignment. The empirical VTF equation

$$\sigma(T) = \frac{A}{\sqrt{T}} \exp\left[\frac{-E_a}{k(T-T_0)}\right] \quad (2)$$

describes its conductivity, with a pseudoactivation energy $E_a \approx$ 0.10 eV and a characteristic temperature T_0 = –74 °C, which is

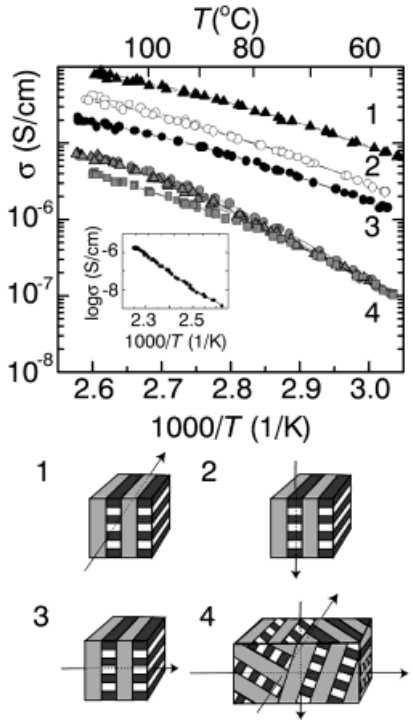

Fig. 4. Direct-current conductivity of PS-*block*-P4VP(TSA)$_{1.0}$(PDP)$_{1.0}$ as a function of temperature. The inset shows the conductivity of the pristine P4VP(TSA)$_{1.0}$, which is poor due to crystallinity. For the non-aligned PS-*block*-P4VP(TSA)$_{1.0}$(PDP)$_{1.0}$ (case 4), the protonic conductivity is improved and isotropic, due to the polydomain structure with different local orientations of the conducting nanowires. In the aligned case (cases 1–3), the protonically conducting nanowires have common overall orientations due to the nearly monodomain structure. The conductivity is increased further due to fewer domain boundaries and the nanoscale conductivity anisotropy is manifestly present.

typically related to the glass transition temperature. In the nonaligned case, the conductivity is isotropic in all three directions with $E_a \approx$ 0.15 eV as the local anisotropies have been averaged out due to the polydomain structure. Interestingly, Figure 4 further shows that upon macroscopic alignment the conductivities in the three directions still increase, possibly due to enhancement of organization of nanostructure and reduction of domain boundaries. The conductivity is anisotropic and highest along the macroscopically aligned protonically conducting nanoscale wires. Lower values are observed for the direction across the relatively thin (order of magnitude 20 Å) insulating pentadecyl layers. The lowest values, however, are observed in the direction across the relatively thick PS layers (order of magnitude 150 Å). This is in good agreement with the structural information from SAXS experiments (Fig. 4).

In order to analyze the proton-hopping transport in more detail, it is helpful first to consider the homopolymeric supramolecules P4VP(TSA)$_{1.0}$(PDP)$_{1.0}$. This material was also oriented by shear flow and characterized using SAXS, see Figure 3. Peaks at q_2 = 0.15 Å^{-1} and $2q_2$ indicate lamellar order with a periodicity of 41 Å, see also Figure 1A. Figure 3 further shows that the conducting lamellae are well oriented along the shearing planes. Also in this case, the conductivity is drastically improved in comparison with the pristine

  0935-9648/02/0503-0359 $ 17.50+.50/0

ADVANCED MATERIALS

P4VP(TSA)$_{1.0}$; at 80 °C the conductivity along the two lamellar directions was 8×10^{-4} S cm^{-1} and that across the insulating pentadecyl layers was slightly lower (3×10^{-4} S cm^{-1}). The conduction activation energies for P4VP(TSA)$_{1.0}$-(PDP)$_{1.0}$ and PS-*block*-P4VP(TSA)$_{1.0}$(PDP)$_{1.0}$ are comparable. Finally, the hopping rates ω_p were evaluated by applying the scaling law:[51] $\sigma(\omega) = \sigma(0)+A\omega^n$ to the higher frequency data, see the insets of Figures 5A and 5B. The hopping rates of the mobile species were evaluated using $\omega_p = [\sigma(0)/A]^{1/n}$,[52] see Figure 5A. For P4VP(TSA)$_{1.0}$(PDP)$_{1.0}$, the hopping rates along the protonically conducting nanoscale layers are an order of magnitude larger than across the pentadecyl insulating layer, see Figure 5A. In agreement, in PS-*block*-P4VP(TSA)$_{1.0}$-(PDP)$_{1.0}$, the hopping rate is decreased by roughly an order of magnitude across the thin pentadecyl layers and still another order of magnitude across the thicker PS layers, see Figure 5B. Therefore, the local tridirectional anisotropy of the nanostructures is directly reflected in the macroscopic conductivity.

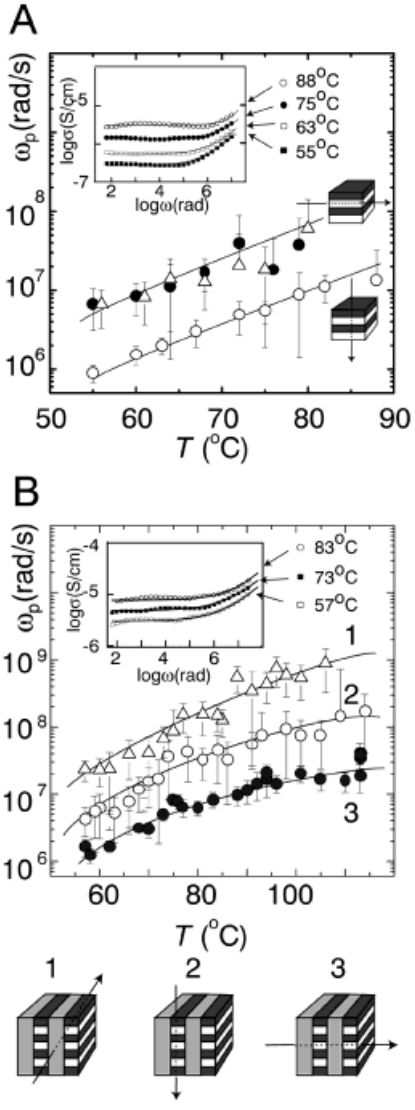

Fig. 5. Hopping rates for the protonic conductivity. A) For P4VP(TSA)$_{1.0}$-(PDP)$_{1.0}$, the hopping rate within the nanoscale lamellae consisting of P4VP(TSA)$_{1.0}$ is an order of magnitude larger than across the thin pentadecyl alkyl layers. B) For PS-*block*-P4VP(TSA)$_{1.0}$(PDP)$_{1.0}$, the largest hopping rate is similarly observed along the nanoscale wires (△, case 1). The hopping rate is reduced an order of magnitude across the insulating pentadecyl alkyl layers (○, case 2) and another order of magnitude further into the third direction where the hopping should take across the thick polystyrene layers (●, case 3).

In conclusion, specific acid–base supramolecules were constructed and the presence of attractive and repulsive interactions renders local nanoscale conducting domains due to self-organization. The number of domain boundaries can be reduced by macroscopic alignment of the local nanostructures, which in this work has been accomplished by an imposed shear flow; plasticized materials with improved protonic conduction were obtained. The nanoscale structures allow tuning of the protonic transport, as two-dimensional nanostructures provide conductivity anisotropy in two dimensions and three-dimensional nanostructures achieve the same in three dimensions. Thus, the molecular level anisotropy is reflected in the macroscopic conductivity behavior in a controlled way.

Experimental

Materials and Sample Preparation: P4VP was obtained from Polyscience Inc. with M_n = 50 000 g mol^{-1}. PS-*block*-P4VP (PS 40 000 g mol^{-1}, P4VP 5600 g mol^{-1}), was obtained from Polyscience Inc. with polydispersity 1.09. PDP was purchased from Aldrich (purity 98 %) and was twice recrystallized with petroleum ether and dried at 40 °C in vacuum for four days before use. TSA was obtained from Acros (purity 98 %). A lamellar-within-lamellar structure was obtained by dissolving PS-*block*-P4VP in analytical grade dimethylformamide (DMF) at 60 °C. A stoichiometric amount (with respect to the number of pyridine groups) of PDP and TSA was added to the dilute solution (1–2 wt.-%). At the end, DMF was evaporated and the sample was vacuum dried (80 °C, 0.04 mbar, 24 h) and stored in a desiccator. Other details of sample preparation, including the preparation of the sample pills for rheological tests, have been described elsewhere [41].

Dynamic Rheology: Oscillatory shear flow using a dynamic rheometer (TA Instruments R1000N) with cone and plate geometry was used (diameter 20 mm, cone angle 4°). Firstly the samples were heated to 130 °C to obtain a homogenous sample with good contact with both the rotor and the stator of the rheometer. Oscillatory shear flow parameters were chosen in agreement with previous work on PS-*block*-P4VP(PDP)$_{1.0}$ [41,53]. After imposing shear flow, the samples were cooled below 0 °C with liquid nitrogen and removed from the rheometer.

Small-Angle X-ray Scattering: The resulting structure was inspected with SAXS (Bruker NanoSTAR); a ceramic fine-focus X-ray tube is used in a point focus mode. The tube is powered with a generator (Kristalloflex K760) at 35 kV and 40 mA. The primary beam is collimated with cross-coupled Göbel mirrors and a pinhole of 0.1 mm in diameter providing a Cu Kα radiation beam (λ = 1.54 Å) with a full-width half-maximum value of about 0.2 mm at the sample position. The sample–detector distance was varied from 0.64 to 1.08 m. A position-sensitive area detector (Siemens-AXS Hi-Star) allowed the scattering intensity to be recorded in the q range 0.08–3 nm^{-1}.

Conductivity Measurements: The conductivities were studied with a Hewlett-Packard HP4192LF Impedance Analyzer at frequencies of 10–10^7 Hz. The P4VP(TSA)$_{1.0}$ and PS-*block*- P4VP(TSA)$_{1.0}$(PDP)$_{1.0}$ were vacuum dried before measurement (60 °C, 0.04 mbar, 24 h) and afterwards stored in a dessicator. In the measurement setup, the sample (typical size about 1×1×2 mm^3) was placed between two platinum plates. The sample was surrounded with Teflon in order to isolate the material from atmospheric humidity and reduce development of defects while measuring above the material's T_g.

The complex impedance plot (resistance versus reactance) showed typical semicircular behavior. The conductivity of the sample was determined based on the intermediate frequency plateau, near 1 kHz, where the electrode interface polarization does not play a major role, for examples see the inset of Figure 5A.

For the temperature sweep, a modified instrument (Linkam TMS 91) was used with heating and cooling rate of 1 K min^{-1} first from 60 to 115 °C and another cycle to 140 °C for PS-*block*-P4VP(TSA)$_{1.0}$(PDP)$_{1.0}$. For P4VP-

  0935-9648/02/0503-0360 $ 17.50+.50/0

$(TSA)_{1.0}(PDP)_{1.0}$, the heating cycle was first 1 K min^{-1} from 50 to 110 °C and another cycle from 60 to 170 °C, which is well above the order–disorder temperature, T_{ODT} = 135 °C. For the P4VP$(TSA)_{1.0}$ salt the heating cycle was from 60 to 170 °C.

Received: August 13, 2001

[1] M. Muthukumar, C. K. Ober, E. L. Thomas, *Science* **1997**, *277*, 1225.
[2] T. A. Skotheim, R. L. Elsenbaumer, J. R. Reynolds, in *Handbook of Conducting Polymers* (Eds: T. A. Skotheim, R. L. Elsenbaumer, J. Reynolds), Marcel Dekker, New York **1998**.
[3] F. M. Gray, *Polymer Electrolytes*, VCH, Weinheim, **1991**.
[4] R. I. Stankovic, R. W. Lenz, F. E. Karasz, *Eur. Polym. J.* **1990**, *26*, 359.
[5] R. I. Stankovic, R. W. Lenz, F. E. Karasz, *Eur. Polym. J.* **1990**, *26*, 675.
[6] S. Kempf, H. W. Rotter, S. N. Magonov, W. Gronski, H. J. Cantow, *Polym. Bull. (Berlin)* **1990**, *24(3)*, 325.
[7] S. Kempf, W. Gronski, *Polym. Bull. (Berlin)* **1990**, *23*, 403.
[8] K. Ishizu, Y. Yamada, R. Saito, T. Yamamoto, T. Kanbara, *Polymer* **1992**, *33*, 1816.
[9] K. Ishizu, Y. Yamada, R. Saito, T. Kanbara, T. Yamamoto, *Polymer* **1993**, *34*, 2256.
[10] K. Ishizu, K. Honda, T. Kanbara, T. Yamamoto, *Polymer* **1994**, *35(22)*, 4901.
[11] J. Li, I. M. Khan, *Makromol. Chem.* **1991**, *192*, 3043.
[12] L. Dai, J. W. White, *Polymer* **1997**, *38*, 775.
[13] B. H. Sohn, R. E. Cohen, *J. Appl. Polym. Sci.* **1997**, *65*, 723.
[14] K. Yoshino, S. Nakajima, R.-I. Sugimoto, *Jpn. J. Appl.Phys.* **1987**, *6*, L2046.
[15] T. J. Prosa, M. J. Winokur, J. Moulton, P. Smith, A. J. Heeger, *Macromolecules* **1992**, *25*, 4364.
[16] G. Wegner, *Makromol. Chem., Macromol. Symp.* **1986**, *1*, 151.
[17] T. Vahlenkamp, G. Wegner, *Macromol. Chem. Phys.* **1994**, *195*, 1933.
[18] H. Sirringhaus, P. J. Brown, R. H. Friend, M. M. Nielsen, K. Bechgaard, B. M. W. Langeveld-Voss, A. J. H. Spiering, R. A. J. Janssen, E. W. Meijer, P. Herwig, D. M. de Leeuw, *Nature* **1999**, *401*, 685.
[19] J. H. Schön, A. Dodabalapur, Z. Bao, C. Kloc, O. Schenker, B. Batlogg, *Nature* **2001**, *410*, 189.
[20] H. Kosonen, J. Ruokolainen, M. Knaapila, M. Torkkeli, K. Jokela, R. Serimaa, G. ten Brinke, W. Bras, A. P. Monkman, O. Ikkala, *Macromolecules* **2000**, *33*, 8671.
[21] J. R. M. Giles, F. M. Gray, J. R. MacCallum, C. A. Vincent, *Polymer* **1987**, *28*, 1977.
[22] P. Lobitz, H. Füllbier, A. Reiche, J. C. Illner, H. Reuter, S. Höring, *Solid State Ionics* **1992**, *58*, 41.
[23] I. M. Khan, D. Fish, Y. Delaviz, J. Smid, *Makromol. Chem.* **1989**, *190*, 1069.
[24] P. V. Wright, Y. Zheng, D. Bhatt, T. Richardson, G. Ungar, *Polym. Int.* **1998**, *47*, 34.
[25] P. P. Soo, B. Huang, Y.-I. Jang, Y.-M. Chiang, D. R. Sadoway, A. M. Mayes, *J. Electrochem. Soc.* **1999**, *146*, 32.
[26] U. Lauter, W. H. Meyer, G. Wegner, *Macromolecules* **1997**, *30*, 2092.
[27] T. Ohtake, M. Ogasawara, K. Ito-Akita, N. Nishina, S. Ujiie, H. Ohno, T. Kato, *Chem. Mater.* **2000**, *12*, 782.
[28] T. Ohtake, Y. Takamitsu, K. Ito-Akita, K. Kanie, M. Yoshizawa, T. Mukai, H. Ohno, T. Kato, *Macromolecules* **2000**, *33*, 8109.
[29] A.-V. G. Ruzette, P. P. Soo, D. R. Sadoway, A. M. Mayes, *J. Electrochem. Soc.* **2001**, *146*, A537.
[30] K. D. Kreuer, *Chem. Mater.* **1996**, *8*, 610.
[31] N. Agmon, *Chem. Phys. Lett.* **1995**, *244*, 456.
[32] M. Eikerling, A. A. Kornyshev, A. M. Kuznetsov, J. Ulstrup, S. Walbran, *J. Phys. Chem. B* **2001**, *105*, 3646.
[33] M. Antonietti, M. Neese, G. Blum, F. Kremer, *Langmuir* **1996**, *12*, 4436.
[34] M. Antonietti, M. Maskos, F. Kremer, G. Blum, *Acta Polymer* **1996**, *47*, 460.
[35] J. Kerres, A. Ullrich, F. Meier, T. Häring, *Solid State Ionics* **1999**, *125*, 243.
[36] M. Rikukawa, K. Sanui, *Prog. Polym. Sci.* **2000**, *25(10)*, 1463.
[37] J.-M. Lehn, *Supramolecular Chemistry*, VCH, Weinheim, **1995**.
[38] J. Ruokolainen, R. Mäkinen, M. Torkkeli, R. Serimaa, T. Mäkelä, G. ten Brinke, O. Ikkala, *Science* **1998**, *280*, 557.
[39] Z.-R. Chen, J. A. Kornfield, S. D. Smith, J. T. Grothaus, M. M. Satkowski, *Science* **1997**, *277*, 1248.
[40] J. Sänger, W. Gronski, H. Leist, U. Wiesner, *Macromolecules* **1997**, *30*, 7621.
[41] R. Mäkinen, J. Ruokolainen, O. Ikkala, K. de Moel, G. ten Brinke, W. de Odorico, M. Stamm, *Macromolecules* **2000**, *33*, 3441.
[42] G. Hadziioannou, A. Mathis, A. Skoulios, *Colloid Polym. Sci.* **1979**, *257*, 136.
[43] K. A. Koppi, M. Tirrell, F. S. Bates, *J. Phys. II* **1992**, *2*, 1941.
[44] J. Ruokolainen, G. ten Brinke, O. T. Ikkala, *Adv. Mater.* **1999**, *11*, 777.
[45] T. Thurn-Albrecht, R. Steiner, J. DeRouchey, C. M. Stafford, E. Huang, M. Bal, M. Tuominen, C. J. Hawker, T. P. Russell, *Adv. Mater.* **2000**, *12*, 787.
[46] K. Ishizu, T. Fukuyama, *Macromolecules* **1989**, *22*, 244.
[47] W. Wieczorek, S. H. Chung, J. R. Stevens, *J. Polym. Sci., Part B: Polym. Phys.* **1996**, *34*, 2911.
[48] N. Binesh, S. V. Bhat, *J. Polym. Sci., Part B: Polym. Phys.* **1998**, *25*, 1201.
[49] S. H. Chung, K. Such, W. Wieczorek, J. R. Stevens, *J. Polym. Sci., Part B: Polym. Phys.* **1994**, *32*, 2733.
[50] M. J. C. Plancha, C. M. Rangel, C. A. C. Sequeira, *Solid State Ionics* **1992**, *58*, 3.
[51] K. A. Jonscher, *Nature* **1977**, *267*, 673.
[52] D. P. Almond, G. K. Duncan, A. R. West, *Solid State Ionics* **1983**, *8*, 159.
[53] R. Mäki-Ontto, K. de Moel, W. de Odorico, J. Ruokolainen, M. Stamm, G. ten Brinke, O. Ikkala, *Adv. Mater.* **2001**, *13*, 117.

Energy Transfer in Mixtures of Water-Soluble Oligomers: Effect of Charge, Aggregation, and Surfactant Complexation**

By *Martin Stork*, *Brent S. Gaylord*, *Alan J. Heeger*, and *Guillermo C. Bazan**

Emissive conjugated polymers are under intense investigation for their potential role in chemical[1] and biological[2] sensors. Intrachain and interchain energy transfer processes[3] allow excitations to sample multiple environments.[4] If one of these sites is in close proximity to a fluorescence quencher molecule, the result is an enhancement of the quenching event. If removal of the quencher molecule from the vicinity of the conjugated polymer can be coupled to the presence of a target analyte, one obtains the platform for optical sensing. It is difficult for isolated fluorophores to exhibit similar amplification.

Water-soluble conjugated polymers[5] are of particular interest in biosensor schemes.[6] To compensate for the hydrophobic nature of the backbone, these polymers contain charged groups for solubility in aqueous media. The dependence of interchain aggregation and the coil conformation show behavior typical of polyelectrolytes. Indeed, many of the lessons learned from the complexation of surfactants to polyelectrolytes[7] have been used to tune the optical properties of polymers such as poly(2,5-methoxy-propyloxysulfonate phenylenevinylene) (MPS–PPV).[8] The relationship between the charge of the quencher molecule and the efficiency of quenching has also been studied for a polymer similar to MPS–PPV.[9]

[*] Prof. G. C. Bazan, Dr. M. Stork, B. S. Gaylord, Prof. A. J. Heeger
Departments of Chemistry and Materials
University of California
Santa Barbara, CA 93106 (USA)
E-mail: bazan@chem.ucsb.edu

[**] This work was funded by the MRL Program of the NSF under Award No. DMR 96-32716 and the Office of Naval Research. This work was supported by a fellowship within the Postdoctoral Program of the German Academic Exchange Service (DAAD). Useful discussions with Prof. Dave Whitten and Dr. Deli Wang are gratefully acknowledged.

  0935-9648/02/0503-0361 $ 17.50+.50/0